α-cluster structure in ^{19}F and ^{19}Ne in resonant scattering

V. Z. Goldberg [1] A. K. Nurmukhanbetova [2] A. Volya [3,1,*] D. K. Nauruzbayev [4,5]
G. E. Serikbayeva [5] and G. V. Rogachev [1,6,7]

[1]*Cyclotron Institute, Texas A&M University, College Station, Texas 77843-3366, USA*
[2]*Energetic Cosmos Laboratory, Nazarbayev University, Nur-Sultan, 010000, Kazakhstan*
[3]*Department of Physics, Florida State University, Tallahassee, Florida 32306-4350, USA*
[4]*Nazarbayev University Research and Innovation System, Nur-Sultan, 010000, Kazakhstan*
[5]*Physics Department, School of Sciences and Humanities, Nazarbayev University, Nur-Sultan, 010000, Kazakhstan*
[6]*Department of Physics and Astronomy, Texas A&M University, College Station, Texas, 77843, USA*
[7]*Nuclear Solutions Institute, Texas A&M University, College Station, Texas 77843, USA*

The nuclear structure of ^{19}F and ^{19}Ne is important for understanding of α clustering in the $A = 20$ mass region and in questions related to astrophysics. However, the only high-resolution broad angular and energy range study of the ^{19}F resonance structure in $\alpha + ^{15}$N scattering was published over 60 years ago, and a detailed analysis of complex excitation functions of overlapping resonances with several decay channels was simply impossible at that time. We performed a modern R-matrix analysis of these old data to assign spins and specify resonant parameters of levels up to excitation energy of 8.2 MeV in ^{19}F. We successfully tested our R-matrix parameters in a fit of the recent data on $\alpha + ^{15}$N obtained by thick target inverse kinematics (TTIK) method at 180 degrees. We used the new parameters for ^{19}F to fit TTIK data for $\alpha + ^{15}$O, the mirror resonant reactions. The comparison of the data for isobaric mirror resonant reactions provides an interesting insight into the nuclear structure.

I. INTRODUCTION

The mirror symmetry between protons and neutrons is both a remarkable and useful property in nuclear physics. Manifestation of this symmetry in clustering resonances is of a particular interest for many present-day theoretical questions, as a tool in evaluation of experimental data, and more broadly in astrophysics, mesoscopic quantum science, and related fields.

Recent development of rare beams opened new possibilities for studies of mirror resonant reactions. In this work we present new data on ^{19}F and ^{19}Ne structure, looking at the corresponding resonant data for ^{15}N $+\alpha$ and ^{15}O $+\alpha$ processes. The ^{19}F and ^{19}Ne are important nuclei for study of clustering structure near mass $A = 20$. In particular, their structure can be compared with ^{20}Ne (^{16}O $+\alpha$) and ^{21}Ne (^{17}O $+\alpha$) [1], exploring the role of an extra nucleon and a nucleon hole relative to ^{16}O core. Both nuclei and the mirror symmetry between the structures of ^{19}Ne and ^{19}F are also important for some questions in astrophysics. Fluorine, for example, is very easily destroyed in stellar interiors and, therefore, has to be deposited into the interstellar medium soon after its production. Because of fluorine's sensitivity to the conditions of its production site, the abundance of cosmic fluorine puts a severe constraint not only on the chemical evolution models describing different stellar populations but also on stellar evolution models [2].

The main existing nuclear physics uncertainty affecting model predictions of the ^{18}F yield in astrophysics arises from the ^{18}F $+ p \rightarrow {}^{19}$Ne $\rightarrow \alpha + {}^{15}$O reaction rate [3,4]. Finally, the dependence of the mirror-energy shift on the position of the α threshold is of significant theoretical interest.

We report below an R-matrix analysis of the old data of the $\alpha + ^{15}$N [5] resonance scattering using modern approach with the help of the AZURE code. Before our work, these classical measurements were treated several times [6], but have never been analyzed in the whole angular and energy region. In addition to that, to further expand the angular reach of the measurements [5], we performed measurements of the $\alpha + ^{15}$N excitation functions for elastic scattering at angles close to 180° c.m. using the TTIK method. Some results of the analysis of these data were reported in the preceding article [7]. In this work we also tested our R-matrix analysis using another source of TTIK data from Ref. [8]. The data in Ref. [8] was obtained at about 40 MeV incident energy of ^{15}N beam, and therefore enable study of ^{19}F at higher excitation energies. A new R-matrix analysis that is based on a more complete data, including that of isobaric partners, helps us to better treat complex interference of resonances and assign and validate spin assignments, thus extending our knowledge of resonant structure in ^{19}F and ^{19}Ne.

This work is a part of the studies of ^{19}F reported in the preceding paper [7] and a new analysis of the excitation function for ^{15}O(α, α) elastic scattering measured in Ref. [9]. These experimental data for ^{19}Ne were reanalyzed using the ^{19}F analysis and mirror comparisons were made. This work is
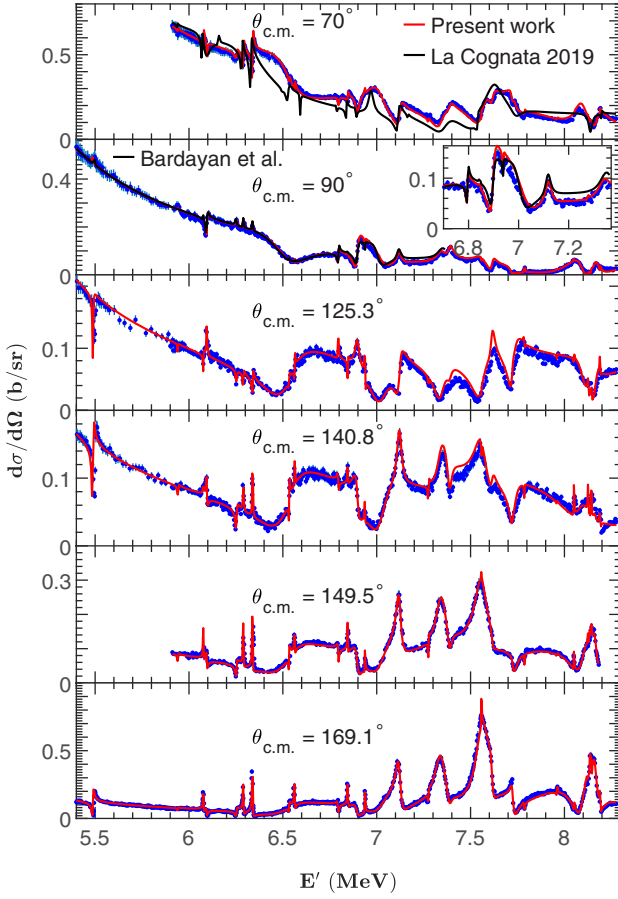
*volya@phy.fsu.edu

FIG. 1. Excitation functions for the $\alpha + {}^{15}$N elastic scattering [5] and R-matrix fit. See text for explanations. Top panel for 70° compares our calculations to those with parameters from La Cognata 2019 in Ref. [8]; the next panel for 90° includes comparison with the fit with parameters of Bardayan *et al.* in Ref. [6]; inset magnifies the area around 7 MeV.

also a part of a broader effort to address α clustering questions in mass $A = 20$ region.

II. *R*-MATRIX ANALYSIS

The $\alpha + {}^{15}$N excitation functions for the elastic scattering in Ref. [5] are presented in Fig. 1. The energy resolution was about 0.1% of the beam energy. The average overall rms error on the measured cross sections is estimated at 6.2%. The digital data of Ref. [5] are available at the EXFORE library [10]. More details of the measurements one can find in the original publication and in the preceding article [7].

We have analyzed these experimental results using the R-matrix code AZURE. To describe the experimental data we used AZURE convolution with experimental resolution of $\sigma = 1.95$ keV. Figure 1 shows the comparison of the excitation functions for the $\alpha + {}^{15}$N elastic scattering from Ref. [5] with our R-matrix fit. Tables I and II summarize the resonance parameters of the present work. Table I covers the excitation region up to 7.3 MeV, which is up to the final resonant peak of the analysis [6]. This table also includes results of the analysis reported in our previous paper [7], which targeted low energies, and the data from compilation in Ref. [11]. The α cluster reduced width, γ_α, see Ref. [7], are also shown for several states.

Most of our newly determined resonance parameters in Table I agree with these of Ref. [6]; some differences in the region below 6.6 MeV of the excitation energy in ^{19}F were discussed in Ref. [7]. As is seen in Table I, we assigned spin $5/2^-$ to the 6.896 MeV resonance and $5/2^+$ to the 7.35 MeV resonance. For both of these the assigned orbital angular momentum of the captured α particle is the same as in Ref. [6]. Therefore the interference with nearby states is similar at 169°. Unfortunately, the authors of Ref. [6] performed the analysis of the available data only for this angle. Considering

TABLE I. ^{19}F levels.

Ref. [6]			Ref. [11]		Present work and Ref. [7]			
E' (MeV)	J^π	Γ_α (keV)	E' (MeV)	Γ_α (keV)	E' (MeV)	J^π	Γ_α (keV)	γ_α
—	—	—	—	—	5.333	$1/2^+$	1.4±0.4	0.60
5.496	$3/2^+$	3.2	5.501	4	5.488	$3/2^+$	4.85±0.5	0.82
6.077	$7/2^+$	1.2	6.070	1.2	6.077	$7/2^+$	0.9	0.2
6.094	$3/2^-$	3.9	6.088	4	6.095	$3/2^-$	3.9	—
6.250	$1/2^+$	7.9	6.255	8	6.253	$1/2^+$	7.5	—
6.289	$5/2^+$	2.4	6.282	2.4	6.289	$5/2^+$	2.30±0.5	0.28
6.338	$7/2^+$	3.6±0.4	6.330	2.4	6.338	$7/2^+$	3.30±0.4	0.28
6.535	$3/2^+$	1.2±0.4	6.528	4	6.534	$3/2^+$	1.5	—
6.536±0.005	$1/2^-$	245±6	6.429	280	6.54	$1/2^-$	220±40	0.51
6.563	$7/2^+$	0.3±0.2	6.554	1.6	6.563	$7/2^+$	0.9	0.04
6.796	$3/2^-$	4.3±0.5	6.787	—	6.795	$3/2^-$	4.2±0.5	—
6.845	$5/2^+$	1.2	6.838	1.2	6.845	$5/2^+$	1.4	—
6.896±0.002	$3/2^-$	22±2	6.891	28	6.896	$5/2^-$	28±4	—
6.938	$7/2^-$	0.9±0.2	6.927	2.4	6.937	$7/2^-$	1.4	—
7.028±0.004	$1/2^-$	96±6	6.989	51	7.048	$1/2^-$	150±35	—
7.118±0.004	$5/2^+$	25±4	7.114	32	7.12	$5/2^+$	30	0.31
7.353	$7/2^+$	65	—	—	7.349	$5/2^+$	73	0.45

TABLE II. ¹⁹F levels above 7.3 MeV excitation energy.

Present work				Ref. [8]		
E' (MeV)	J^π	Γ_α (keV)	γ_α	E' (MeV)	J^π	Γ_α (keV)
7.349	$5/2^+$	73	0.45	7.364	$5/2^+$	99.9
7.390	$1/2^+$	30	—	—	—	—
(7.558)	$5/2^+$	1.1	—	7.539	$5/2^+$	12.0
7.564	$7/2^+$	82	0.49	7.56	$7/2^+$	158
7.612	$3/2^-$	25	—	—	—	—
7.723	$3/2^-$	16	—	—	—	—
7.737	$1/2^-$	50	—	7.702	$1/2^-$	327
(7.786)	$(5/2^-)$	2.4	—	7.74	$5/2^-$	73.7
7.980	$5/2^-$	255	—	7.929	$7/2^+$	263
(8.051)	$(5/2^+)$	0.65	—	8.084	$9/2^-$	8.06
(8.126)	$(7/2^-)$	1.05	—	—	—	—
(8.134)	$(7/2^+)$	0.5	—	8.138	$1/2^+$	1008
(8.144)	$(7/2^-)$	1.0	—	8.138	$11/2^+$	22.2
8.152	$3/2^-$	80	—	—	—	—
(8.191)	$9/2^-$	1.4	—	8.199	$5/2^+$	35.9
8.29	$1/2^-$	470	—	8.288	$13/2^-$	2.14
8.34	$3/2^-$	370	—	8.310	$5/2^+$	3.59
8.54	$5/2^-$	330	—	8.374	$7/2^+$	10.9
8.55	$1/2^+$	250	—	—	—	—
8.62	$3/2^+$	250	—	8.591	$3/2^-$	659

other angles where contribution of the $5/2^-$ is generally larger and that of $5/2^+$ is smaller, greatly improves the fit (χ^2 is several times smaller), see Fig. 1, 90°.

The R-matrix analysis is more complicated at higher excitation energies in ¹⁹F. This is because of higher level density and lack of previous studies. Table II summarizes parameters of the resonances from the present fit and from Ref. [8].

La Cognata *et al.* [8] performed TTIK measurements of the $\alpha+$¹⁵N excitation functions for the elastic scattering and made the fit using AZURE code. The authors [8] focus on the data corresponding to α particles emitted at backward angles, close to 180 c.m. since they show a better resolution; they also were interested in strong α cluster resonances. First, we tested a description of the excitation functions [10] using parameters [13]. As one can see in Fig. 1, at 70° it appears that the parameters [8] do not fit the data [5] well. Similar disagreements are seen for most angles of the measurements [5]. Second, we tested how our parameters fit data [8]. Figure 2 shows the excitation functions for the $\alpha+$¹⁵N elastic scattering measured by the TTIK method. It seen that both measurements [8] and [7] are in good agreement with each other. As seen in Fig. 2, our R-matrix parameters, which fit data [5] provide also for a good description of the TTIK data of Ref. [8] at 180°. In the R-matrix fit (Fig. 2) we convoluted the calculations with 33 keV experimental energy resolution of data [7]. Probably fit to data [8] would be even better if a somewhat larger energy resolution parameter were used in the convolution.

Table II presents the resonance parameters of this work in comparison with these of Ref. [8]. A few narrow resonances in the excitation energy region over 8.0 MeV are tentative, and we put them in parentheses. These narrow resonances should not influence the fit [8] because of insufficient energy
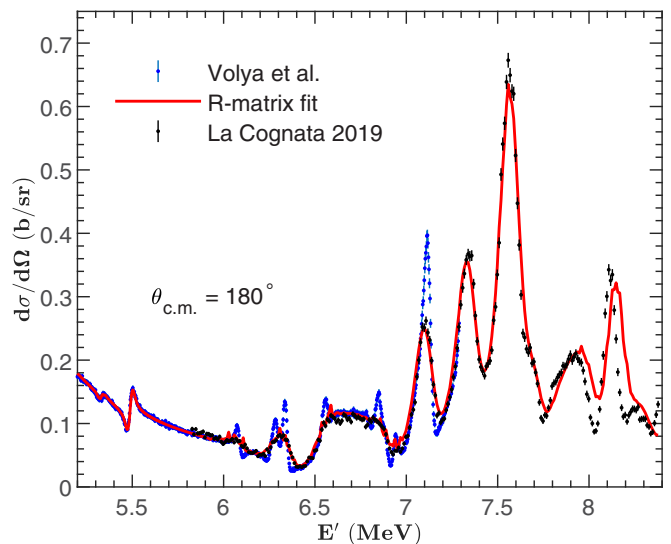

FIG. 2. Excitation functions for the $\alpha+$¹⁵N elastic scattering measured by the TTIK approach (Volya *et al.* [7] and La Cognata 2019 [8]) and R-matrix fit. See text for details.

resolution in the experiment. As seen in Table II in the region between 7.3 and 8.0 MeV, the majority of our spin assignments support those of Ref. [8]; both assign $5/2^+$ to the level at 7.3 MeV.

Most of the differences between the parameters of the present work and those of Ref. [8] are related to the interpretation of the peak at the excitation energy of 8.15 MeV in ¹⁹F (Figs. 1, 2). The authors of Ref. [8] have attributed the peak to a contribution from $11/2^+$ level. Evidently, the assignment of $11/2^+$ is in contradiction with the measurements [5] (see Fig. 1, 70°). In addition to that, the α width of the $11/2^+$ used in the fit [8] seems to be too large. This width is more than three times above the Wigner limit. In contrast to that interpretation, our fit relies on a complicated combination of broad and narrow resonances. Because of this it is difficult to consider and present a clear-cut evidence for the parameters of each resonant level separately. From our search for the best fit, it is certain that the region in question is not dominated by a contribution of one or even two levels; it is a more complicated structure. Another example of discrepancy with the fit [8] is a broad level at 7.9 MeV. Authors of Ref. [8] assigned orbital momentum $\ell = 3$ to the level. The $\ell = 3$ resonance is very small at 90°, and this appears in contradiction with the experimental data [5].

As it is shown in Table II, we included in the fit a few background resonances at the excitation energies above the region covered by the measurements [5]. In this region of background resonances there are no strong peaks, which could influence the results of our fit. The main reason to include the background resonances was to test influence of low spin (broad) resonances beyond the region of the measurements [5]. This test showed that while the included resonances influence the 8 MeV excitation region in ¹⁹F, they do not change the spin assignment. The $\ell = 0$ resonance at 8.32 MeV has the most impact, and its inclusion improved the fit at 90°. This was the reason to move this resonance closer to the

TABLE III. Theoretical results from model in Ref. [7] are compared with experiment. Only broad resonances in ^{20}Ne and ^{19}F in the 3^- channel are included. In addition to spin and parity labels of states include subscript indicating their order in excitation, n stands for the number of nodes in the relative wave function, and SF stands for spectroscopic factor that can roughly be compared with reduced width γ_α. Theory-experiment correspondence can be subjective but other factors such as proton spectroscopic factors were considered for the suggestion presented in the table.

J_i^π	E_{th} (MeV)	n	SF	E_{exp} (MeV)	γ_α
3_2^-	8.255	3	0.354	7.156	1.37
$5/2_5^+$	6.552	2	0.038	6.289	0.28
$5/2_6^+$	7.293	3	0.252	7.120	0.31
$5/2_8^+$	7.631	3	0.012	7.349	0.45
$7/2_3^+$	6.302	2	0.496	6.077	0.20
$7/2_6^+$	8.347	3	0.468	6.338	0.31
$7/2_7^+$	8.632	2	0.218	7.565	0.49

investigated region. Probably, this is an indication for a broad $\ell = 0$ resonance, an analog of the famous broad resonance 0^+ in ^{20}Ne at the excitation energy of 8.77 MeV [12]. A detailed experimental data of this region in ^{19}F and a careful analysis are needed to support this assumption.

We did not see any of the levels observed in the $p+^{18}$O resonant studies, which covered the region up to 8.2 MeV excitation energy in ^{19}F (see Ref. [13] and references therein). These resonances are important for the estimation of synthesis of ^{19}N, ^{18}O, and ^{19}F isotopes in the $p+^{18}$O interaction in stars. This is likely due to very narrow widths of the levels (less than 200 eV) [13], something that is also supported by the theoretical arguments in Ref. [7].

In the previous article [7], we have noted a remarkable correspondence between the cluster levels in ^{19}F and the well-known α cluster states in ^{20}Ne. Namely, each broad state in ^{20}Ne (seen as ^{16}O $+\alpha$) had a corresponding match in ^{19}F (^{15}N $+\alpha$) with the same cluster-core relative wave function. Because of $1/2^-$ spin parity of ^{15}N (due to a proton hole on $p_{1/2}$ orbit) for nonzero partial waves a spin-orbit doublet is observed. Evidently the situation is somewhat different for $\ell = 3$. In correspondence to a single 3^- state at 7.16 MeV excitation energy and reduced width ≈ 1.4 in ^{20}Ne [12], we have three pairs ($5/2^+$, $7/2^+$) of α cluster states in ^{19}F (see Tables I and II) with a sum of reduced widths ≈ 1. A single 3^- resonance at 7.16 MeV excitation in ^{20}Ne [17] with reduced width ≈ 1.4 in ^{19}F fragments into three pairs ($5/2^+$, $7/2^+$) of α cluster states (see Tables I and II) with a sum of reduced widths of about 1. This observation was not expected in α cluster models (see Ref. [14] and references therein) but is explained by the presence of an extra proton hole in more microscopic models from Ref. [7]. The extra states emerge from ^{15}N $+\alpha$ scattering channel with two nodes in the wave function where effectively one of the nucleons from an α particle occupies a hole in the $p_{1/2}$ orbit in a final state. This channel is Pauli blocked for ^{20}Ne. Table III summarizes theoretical and experimental results for broad α clustered states in ^{20}Ne and ^{19}F in the 3^- channel.
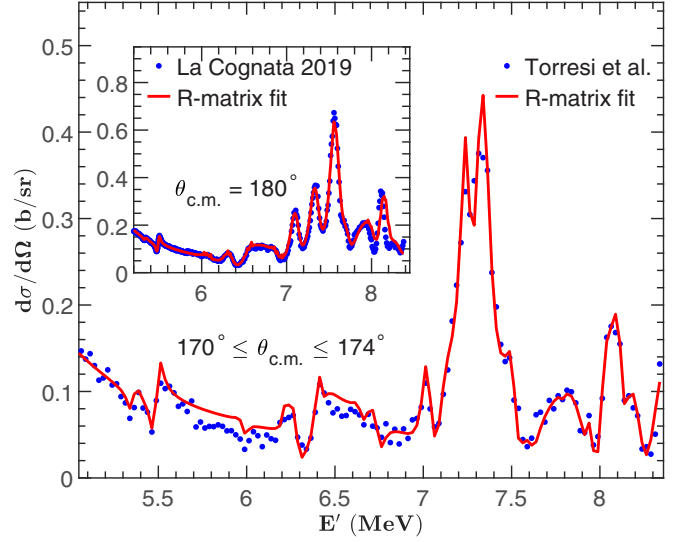

FIG. 3. Excitation function for the $\alpha+^{15}$O elastic scattering, points show data from Torresi *et al*, [9]. Inset shows the mirror excitation function for $\alpha+^{15}$N scattering and data from La Cognata 2019 [8].

III. RESONANCES IN THE MIRROR ^{19}Ne NUCLEUS

For the mirror ^{19}Ne system, the $\alpha+^{15}$O elastic scattering measurements in Ref. [9] were performed at the Laboratori Nazionali di Legnaro (LNL, Italy) by the TTIK method. The energy of the ^{15}O rare beam was 28.5 MeV. The elastic scattering was measured in the 5–9 MeV excitation energy region in ^{19}Ne at a single angle close to $0°$ in the laboratory system ($180°$ c.m.) with energy resolution of (FWHM) ≈ 30 keV. In the original publication [9], it is said that the angle is zero degrees, however, in the data library [10] the angle is $3°$. We used the $3°$ value from the digital data library and observed no significant difference in results if $0°$ were used. Figure 3 shows the $\alpha+^{15}$O excitation function [9].

An original R-matrix fit of Ref. [9] was performed using code AZURE2. As a starting point the authors of Ref. [9] used known parameters of compilation [11] for levels in ^{19}F. However, an analysis of the excitation region of ^{19}F above 7.3 MeV was absent. Therefore the authors of Ref. [9] did not have good initial parameters for the corresponding excitation region in ^{19}Ne and simply varied the spins and parities of the states systematically and compared the goodness of fit. Having obtained an improved data on ^{19}F our next goal is to see if ^{19}F spectrum can be used to further improve ^{19}Ne analysis and simultaneously we can assess if there is some trend when going from ^{19}F to ^{19}Ne, which can be helpful more broadly in similar cases of mirror nuclei.

In order to test the region of several weak tentative resonances in the higher-energy region around 8.3 MeV, we reexamined the fit of data [8]; this also helps the comparison with ^{15}O $+\alpha$ data of the similar experimental approach [9]. Table IV summarizes resulting R-matrix parameters. Comparing the present work ^{19}F parameters of Table II and Table IV one might note minor differences for a few levels below 8 MeV excitation energy. These, we suppose, are the result

TABLE IV. Mirror resonances in ^{19}F and ^{19}Ne.

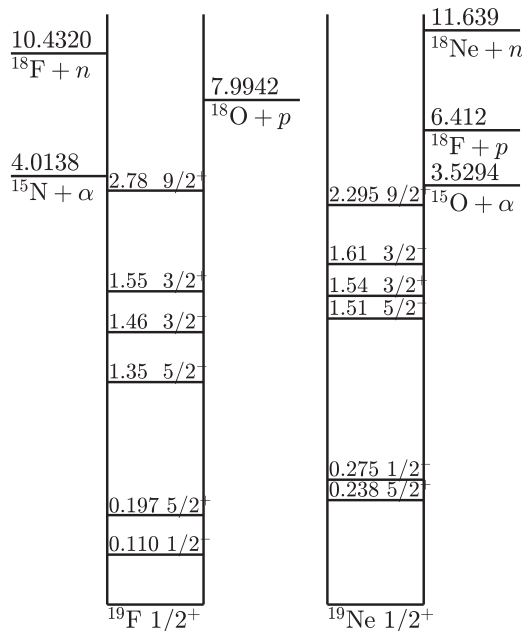| N	Present work (^{19}F)			Present work (^{19}Ne)				Ref. [9]		
	E' (MeV)	J^π	Γ_α (keV)	E' (MeV)	J^π	Γ_α (keV)	ΔE (keV)	E' (MeV)	J^π	Γ_α (keV)
1	5.333	$1/2^+$	1.4	5.355	$1/2^+$	7.0	22	5.359(6)	$1/2^+$	10(3)
2	5.488	$3/2^+$	4.8	5.490	$3/2^+$	12.0	2	5.487(4)	$3/2^+$	9(2)
3	–	–	–	–	–	–	–	5.704(8)	$5/2^-$	29(6)
4	6.095	$3/2^-$	3.9	5.985	$3/2^-$	6.0	−110	5.983(9)	$3/2^-$	21(8)
5	6.253	$1/2^+$	7.5	(6.268)	$1/2^+$	11.0	15	6.197(8)	$1/2^-(1/2^+)$	16(5)
6	6.289	$5/2^+$	2.3	6.233	$5/2^+$	3.6	−56	6.279(2)	$5/2^+$	6(2)
7	6.339	$7/2^+$	3.3	6.272	$7/2^+$	5.5	−67	–	–	–
8	6.540	$1/2^-$	220	6.398	$1/2^-$	135	−142	6.395(5)	$1/2^-$	181(58)
9	6.563	$7/2^+$	0.9	6.415	$7/2^+$	1.6	−148	7.030(4)	$7/2^+$	12(3)
10	6.795	$3/2^-$	4.2	(6.650)	$3/2^-$	4.2	−145	–	–	–
11	6.896	$5/2^-$	28	6.742	$5/2^-$	24	−156	–	–	–
12	7.048	$1/2^-$	150	7.027	$1/2^-$	145	−21	–	–	–
13	7.12	$5/2^+$	30	7.03	$5/2^+$	28	−90	–	–	–
14	–	–	–	7.100	$3/2^+$	13.0	–	7.153(9)	$3/2^+$	233(44)
15	7.349	$5/2^+$	73	7.247	$5/2^+$	29.0	−102	7.469(7)	$5/2^+$	83(17)
16	7.390	$1/2^+$	30	7.026	$1/2^+$	35	−364	–	–	–
17	7.564	$7/2^+$	82	7.343	$7/2^+$	82	−221	7.378(7)	$7/2^+$	121(9)
18	7.612	$3/2^-$	28	7.513	$3/2^-$	35	−101	7.568(2)	$3/2^+(1/2^+)$	774(144)
19	7.723	$3/2^-$	16	–	–	–	–	–	–	–
20	7.737	$1/2^-$	50	7.630	$1/2^-$	40	−107	–	–	–
21	7.785	$5/2^-$	2.4	7.790	$5/2^-$	7.0	4	–	–	–
22	7.980	$5/2^-$	255	7.861	$5/2^-$	240	−137	–	–	–
23	8.134	$7/2^+$	0.5	7.933	$7/2^+$	4.0	−199	–	–	–
24	8.152	$3/2^-$	80	8.103	$3/2^-$	48.0	−49	8.022(4)	$9/2^+$	64(10)
25	8.165	$5/2^-$	200	8.053	$5/2^-$	120.0	−112	–	–	–
26	(8.167)	$(1/2^+)$	22	7.970	$1/2^+$	18	−170	–	–	–
27	8.290	$1/2^-$	470	8.250	$1/2^-$	500	−40	8.223(7)	$5/2^+$	377(34)
28	8.340	$3/2^-$	370	8.18	$3/2^-$	75	−160	–	–	–
29	8.540	$5/2^-$	330	8.50	$5/2^-$	250	−40	–	–	–
30	8.550	$1/2^+$	250	8.45	$1/2^+$	300	−100	–	–	–
31	8.620	$3/2^+$	250	8.45	$3/2^+$	300	−170	–	–	–

of different energy calibration and a poorer resolution of the TTIK approach [8]. At energy over 8 MeV, there is fair agreement for broad levels, however, a more detailed experimental data is needed to resolve several cases with significant differences. Both sets of parameters (Table II and Table IV) provide practically equivalent good description of the data [5].

Because of the mirror symmetry of the processes one expects some correspondence between the resonant $\alpha+^{15}$N and $\alpha+^{15}$O reactions. However, it is well known that the Coulomb interaction, proton-neutron mass difference, and other isospin breaking effects result in some shifting of mirror levels nuclei. Importantly, the thresholds for α particle and proton/neutron decays differ in ^{19}F and ^{19}Ne. Figure 4 shows a low-energy level scheme for ^{19}F and ^{19}Ne and includes the thresholds. We note that the α particle and proton decay thresholds are lower in ^{19}Ne. The dependence of the mirror-energy shift on the position of the threshold (often called the Thomas-Ehrman shift, see [15] and references therein) is well known and results in a decrease of the mirror levels excitation energy in proton-rich nuclei. The single particle s states in proton-rich mirror nuclei are strongly shifted down relative to other states, this is because for a single-particle halolike state the Coulomb

contribution to the energy is significantly reduced. This shift known as Nohlen-Schiffer (NS) effect [16] can be really large ($\approx$1 MeV).

The effect is often observed in the studies of exotic nuclei because of lowering of the s orbit (see, for instance, Ref. [17]). Given that the single-particle reaction continuum plays the main role in the effect the single particle states are of most interest both theoretically and experimentally. It is certainly interesting to look for the same effects in reference to the continuum of α scattering states. Unfortunately, for the states with developed α cluster structure the corresponding information is very scarce because this structure is mainly observed in self-conjugate nuclei such as ^{8}Be, ^{12}C, ^{16}O, ^{20}Ne. There are just a couple of experimental works [18], which noted some peculiar differences in the spectra of mirror resonant reactions.

To evaluate possible effects of near-threshold conditions we used a potential model. We used a Woods-Saxon potential of depth V_0; $R = 3.22$ fm; $a = 0.65$ fm for the ^{18}F $+n$ interaction to calculate ground and excited single-particle states in ^{19}F. The value of V_0 of -68.45 MeV was fit to describe the -10.42 MeV neutron binding energy in ^{19}F (Fig. 4). The

FIG. 4. Scheme of the lowest levels in mirror nuclei ^{19}F and ^{19}Ne.

FIG. 5. ΔE, shift of excitation energies of levels in ^{19}Ne relative to their mirror counterpart in ^{19}F calculated in the potential model (see text for explanations).

potential of a uniformly charge sphere was added to describe the mirror levels in ^{19}Ne. The correct value of the proton binding energy of 6.41 MeV in ^{19}Ne was obtained at the R_c, charge sphere radius, of 3.52 fm. Then the mirror levels in ^{19}F and ^{19}Ne were calculated for orbital momenta of nucleons, $\ell = 0$ and 2, at different values of V_0 (we neglected spin orbital interaction here because it is of little importance for the Coulomb shifts).

In a similar way we calculated the shifts for α cluster states. Assuming α+core interaction is being modeled by a Woods-Saxon potential, we used the values of V_0 that result in a four-node relative wave function for the $\alpha + ^{15}$N (or $\alpha + ^{15}$O), relative motion that corresponds to a $1/2^-$ resonance in ^{19}F with a proper asymptotic α+core relative energy. This is set by a resonant energy relative to the α-decay threshold. This number of the nodes comes from results of the shell model calculations described in the previous article [7], and the cluster character of this state is supported by experimental studies of the α cluster transfer reactions [19]. The value of V_0 and R_c were varied to fit the binding energies of α particles in the mirror $1/2^-$ states, 3.90 MeV in ^{19}F and 3.25 MeV in ^{19}Ne. The final set of parameters is: $V_0 = -135.5$ MeV; $R = 3.03$ fm; $a = 0.6$ fm; $R_c = 5.30$ fm. These nuclear parameters appeared to be close to those used in optical model calculations [20] to describe elastic scattering of α particles on 4N nuclei. The overall binding energy of an α particle depends on the parameters of the nuclear potential and at the same time the difference in binding energies of the mirror states depends primarily on the Coulomb potential.

In Fig. 5, Coulomb shift, ΔE ^{19}Ne, as a function of excitation energies of levels in ^{19}Ne relative their mirror counterparts in ^{19}F is calculated in the framework of the approach described above. These shifts are calculated assuming either single-nucleon or α+core models. It is seen in Fig. 5 that the shift, ΔE ^{19}Ne, is of different sign for the single-particle,
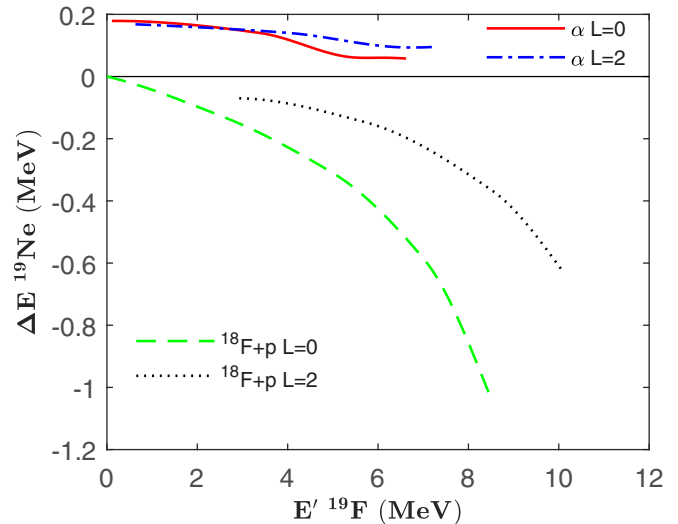
nucleon, and for the α cluster states. The NS effect is evident for the single-particle states in Fig. 5.: the ΔE ^{19}Ne values for $\ell = 0$ are rapidly going down, relative to $\ell = 2$, in the vicinity of the proton decay threshold in ^{19}Ne (6.41 MeV). This effect is much weaker for the α cluster states, evidently, due to a larger mass of the α particle and stronger Coulomb barrier that weakens the continuum coupling, as was noted before in Ref. [21].

The presented calculations suggest that a Coulomb shift can be used to discriminate single-particle and cluster states. States dominated by the single nucleon structure may have a downward shift of ≈ 200 keV in ^{19}Ne; at the same time a smaller shift in the opposite direction may be seen for α cluster levels. In realistic situations given some mixing of configurations the shifts are expected to be smaller.

Figure 3 presents the 170–174° c.m. (the angle increases with the excitation energy) excitation function for the ^{15}O$+\alpha$ elastic scattering from Ref. [9] measured by TTIK method. Inset in Fig. 3, included for comparison, shows the excitation function for the ^{15}N$+\alpha$ elastic scattering also measured by the TTIK method (Fig. 2). These spectra have a few common features. There is a peak at excitation energy of ≈ 8.15 MeV in ^{19}F and a group of peaks at ≈ 8.05 MeV in ^{19}Ne. A peak at 7.55 MeV dominates in the spectrum of ^{19}F, and there is a similar group of peaks in ^{19}Ne at 7.35 MeV. To fit the ^{15}O$+\alpha$ experimental data we used code AZURE. In the ^{19}Ne, in energy excitation region below 7.0 MeV the widths of levels in the fit for ^{19}F were corrected for the different penetrability in ^{19}Ne. Then the excitation energy of each level was variated to fit a corresponding feature in the ^{19}Ne spectrum. A few narrow resonances found in ^{19}F were not used because of the poorer resolution in the ^{19}Ne measurements.

A comparison of both spectra in Fig. 2 indicates a different shifts of ^{19}F major peaks in the region 7.1–7.5 MeV. We found that the most intense peak in ^{19}Ne shifted much stronger to lower energies than the other two. Besides that, the width of

the nearby $5/2^+$ level should be much narrower than could be expected from the ^{19}F fit (see Table IV, #15). Trying to correct the width of the $5/2^+$ level, we have included $3/2^+$ level in ^{19}Ne at 7.08 MeV, which was found in the studies of the ^{18}F$(p, \alpha)^{15}$O cross section at energies of astrophysical interest [3,6]. A mirror level in ^{19}F is not known. The inclusion of this level improves slightly the fit in a region close 7.1 MeV, but does not result in a desirable change of the width of the $5/2^+$ level. (It is interesting that the best fit resulted in the similar total width of $3/2^+$ level as in Ref. [3,6] and in a reverse to given in Ref. [3,6] relation between proton and α widths). We tested other options and found that presence of a relatively weak $\ell = 2$ ($3/2^-$, $5/2^-$) resonance at 7.25 MeV allows us to increase width of $5/2^+$ resonance in question by a factor of two, which slightly improves the fit. However, being unsure about the relation to ^{19}F spectrum, we did not include this hypothetical resonance in the final fit (Table IV).

The structure at 8.15 MeV in ^{19}F is due to an interference of several levels with an unremarkable α particle widths (see Table II). To fit the spectrum of ^{19}Ne we moved these ^{19}F levels down by ≈100 keV; then a small variation of their excitation energies (see Table IV) provided a fit shown in Fig. 3. In addition to that, all broad background resonances at excitation energies above 8.2 MeV in ^{19}F were moved to lower energies in ^{19}Ne, as is shown in Table IV. Several open proton decay channels result in too much freedom for a fit of the limited ^{19}Ne data in this region and, therefore, the parameters of those levels are not strongly fixed.

Table IV allows us to compare our fit parameters with those of the original fit in Ref. [9]. The results of both works are similar up to the excitation energies of 7 MeV in ^{19}Ne. This is understandable, because both fits were mainly based on the analysis of the same ^{19}F data. The only significant difference is in a very strong $5/2^-$ (#3) resonance that comes from the analysis [9]. We checked an inclusion of this resonance in the ^{19}F analysis and found that such strong resonance destroys the fit. At higher excitation energies, the results of both works are different. We attribute this to lack of information that the authors of Ref. [9] had on ^{19}F. In particular, Ref. [9] suggests two very strong α cluster $3/2^+$ (#14 and #18) levels; presence of any of those levels would destroy our ^{19}F fit (as well as the fit [8]). In that energy region only the strongest $7/2^+$ level (#17) is consistent between the current and previous results.

Addressing the shift of mirror levels that comes from our analysis, it is worthwhile to note that the average shift of the ^{19}Ne levels, Δ in Table IV, calculated on 19 resonances up to 7.5 MeV excitation energy in ^{19}F was -101 keV. It is close to the predictions of the potential model for nucleons with orbital momentum different from zero (Fig. 4). There are several cases with significant deviation from the average: (i) Two levels (#1 and #2) with very large reduced α cluster widths have small but positive shifts in accord with calculations shown in Fig. 4. (ii) The shift down of the strongest level $7/2^+$ (#17) is much bigger than the average, and this is a main reason for the change of the ^{19}Ne spectrum. We plan to publish a detailed theoretical analysis elsewhere; preliminary calculations shows that the wave function of this state mainly contains two practically orthogonal parts: the cluster wave function with four nodes and a single particle wave function, a nucleon in an s state plus ^{18}F in the first excited state (3^+). The 7.55 MeV state is well below the corresponding threshold for neutron decay in ^{19}F (11.37 MeV), however, the 7.35 MeV state is exactly at the threshold of the mirror decay in ^{19}Ne. Hence, an idea of the NS effect explains the strong shift down of the mirror level in ^{19}Ne. There is also a strong shift down for $1/2^+$ level (#16). It also might be explained by the NS effect related to the ^{18}F ground state wave function.

IV. CONCLUSIONS

The aim of this work was to obtain new information on ^{19}F and ^{19}Ne nuclear structure from an analysis of the data on resonant scattering $\alpha+^{15}$N and $\alpha+^{15}$O. The sources of data include old data [5], results of our earlier study in Ref. [7] using TTIK approach, and reanalysis of data from the TTIK experiments [8] and [9].

We performed an R-matrix analysis of the high-energy resolution data [5] on $\alpha+^{15}$N elastic scattering up to the excitation energy of 8.2 MeV in ^{19}F. We assigned new spins to a few resonances and specified resonant parameters of several levels. In contrast to an earlier conclusion from Ref. [8], our fit showed that the strong peak at 8.15 MeV excitation energy in ^{19}F at angles close to $180°$ is a result of an interference of several resonances with different (not high) spins. We successfully tested our R-matrix analysis for the $\alpha+^{15}$N elastic scattering obtained at $180°$ c.m. using TTIK approach.

We applied the ^{19}F results to explain excitation function for the $\alpha+^{15}$O elastic scattering obtained by the TTIK method [9], and we found that an interpretation based only on the data obtained for a short angular interval close to 180 degrees in the excitation energy region of many overlapping resonances might be erroneous. This is important because usually experimental data from TTIK approach involving resonant scattering of rare beams are very useful for studies of the lowest states in exotic nuclei. We also showed that a combination of TTIK data for mirror reactions can be useful for obtaining additional spectroscopic information. While the analysis of the Coulomb shifts has a long story, it was mainly used for the lowest single-particle states in mirror nuclei. It was not used in relation to α clustering structure because most data is available only for symmetric $N = Z$ nuclei. The current development of rare beams opens new possibilities for broad studies of cluster-related shifts and their dependence on nuclear structure. Since the energy resolution in the TTIK applications with rare beams is unlikely to be as good as that of classical measurements, it is important to develop methods, which would allow to analyze complete kinematics of resonant processes.

Finally, this work is guided by the theory briefly introduced in the preceding paper [7] and brings a lot of additional input to the models helping in exploration of clustering physics on the verge of stability. However, while some of the new ideas are briefly mentioned, a detailed theoretical analysis discussing mirror symmetry, distribution of widths, and study of the role of nucleon degrees of freedom in clustering around mass 20 region are left for another publication.

[1] A. K. Nurmukhanbetova, V. Z. Goldberg, D. K. Nauruzbayev, M. S. Golovkov, and A. Volya, Evidence for α-cluster structure in ^{21}Ne in the first measurement of resonant ^{17}O$+\alpha$ elastic scattering, Phys. Rev. C **100**, 062802(R) (2019).

[2] A. Best, F. R. Pantaleo, and LUNA collaboration, Low energy cross section of ^{18}O(p, γ) ^{19}F, J. Phys.: Conf. Ser. **1668**, 012002 (2020).

[3] M. La Cognata, R. G. Pizzone, J. Jose, M. Hernanz, S. Cherubini, M. Gulino, G. G. Rapisarda, and C. Spitaleri, A Trojan Horse approach to the production of ^{18}F in novae, Astrophys. J. **846**, 65 (2017).

[4] M. R. Hall, D. W. Bardayan, T. Baugher *et al.*, ^{19}Ne level structure for explosive nucleosynthesis, Phys. Rev. C **102**, 045802 (2020).

[5] H. Smotrich, K. W. Jones, L. C. McDermott, and R. E. Benenson, Elastic scattering of α particles by N^{15}, Phys. Rev. **122**, 232 (1961).

[6] D. W. Bardayan, R. L. Kozub, and M. S. Smith, ^{19}F α widths and the ^{18}F $+$p reaction rates, Phys. Rev. C **71**, 018801 (2005).

[7] A. Volya, V. Z. Goldberg, A. K. Nurmukhanbetova, D. K. Nauruzbayev, and G. V. Rogachev, Phys. Rev. C **105**, 014614 (2022).

[8] M. La Cognata, M. Fisichella, A. Pietro Di, P. Figuera, V. Z. Goldberg, S. Cherubini, J. P. Fernández Garcia, M. Gulino, L. Lamia, D. Lattuada, M. Lattuada, R. G. Pizzone, G. G. Rapisarda, S. Romano, R. Spartá, C. Spitaleri, D. Torresi, A. Tumino, and M. Zadro, Observation of ^{15}N $+\alpha$ resonant structures in ^{19}F using the thick target in inverse kinematics scattering method, Phys. Rev. C **99**, 034301 (2019).

[9] D. Torresi, C. Wheldon Tz. Kokalova, S. Bailey, A. Boiano, C. Boiano, M. Fisichella, M. Mazzocco, C. Parascandolo, D. Pierroutsakou, E. Strano, M. Zadro, M. Cavallaro, S. Cherubini, N. Curtis, A. Di Pietro, J. P. Fernandez-Garcia, P. Figuera, T. Glodariu, J. Grebosz, M. La Cognata, M. La Commara, M. Lattuada, D. Mengoni *et al.*, Evidence for ^{15}O $+\alpha$ resonance structures in ^{19}Ne via direct measurement, Phys. Rev. C **96**, 044317 (2017).

[10] NNDC, Experimental Nuclear Reaction Data (EXFOR).

[11] D. R. Tilley, H. R. Weller, C. M. Cheves, and R. M. Chasteler, Energy levels of light nuclei A = 18–19, Nucl. Phys. A **595**, 1 (1995).

[12] D. K. Nauruzbayev, V. Z. Goldberg, A. K. Nurmukhanbetova, M. S. Golovkov, A. Volya, G. V. Rogachev, and R. E. Tribble, Structure of ^{20}Ne states in resonance ^{16}O $+\alpha$ elastic scattering, Phys. Rev. C **96**, 014322 (2017).

[13] C. G. Bruno *et al.*, Improved astrophysical rate for the ^{18}O(p, α) ^{15}N reaction by underground measurements, Phys. Lett. B **790**, 239 (2019).

[14] R. Otani, R. Kageyama, M. Iwasaki, M. Kudo, M. Tomita, and M. Ito, $\alpha+^{15}$O cluster structure in ^{19}Ne and resonant α scattering, Phys. Rev. C **90**, 034316 (2014).

[15] E. Comay, I. Kelson, and A. Zidon, The Thomas-Ehrman shift across the proton dripline, Phys. Lett. B **210**, 31 (1998).

[16] A. Nolen and J. P. Schiffer, Coulomb energies, Annu. Rev. Nucl. Sci. **19**, 471 (1969).

[17] V. Z. Goldberg, B. T. Roeder, G. V. Rogachev, G. G. Chubarian, E. D. Johnson, C. Fu, A. A. Alharbi, M. L. Avila, A. Banu, M. McCleskey, J. P. Mitchell, E. Simmons, G. Tabacaru, L. Trache, and R. E. Tribble, First observation of ^{14}F, Phys. Lett. B **692**, 307 (2010).

[18] Changbo Fu, V. Z. Goldberg, G. V. Rogachev, G. Tabacaru, G. G. Chubarian, B. Skorodumov, M. McCleskey, Y. Zhai, T. Al-Abdullah, L. Trache, and R. E. Tribble, First observation of α-cluster states in the ^{14}O $+^4$He interaction, Phys. Rev. C **77**, 064314 (2008).

[19] S. Mordechai and H. T. Fortune, Negative-parity α clusters in ^{19}F, Phys. Rev. C **29**, 1765 (1984).

[20] K. O. Behairy, Z. M. M. Mahmoud, and M. Anwar, α-particle elastic scattering from ^{12}C, ^{16}O, ^{24}Mg, and ^{28}Si, Nucl. Phys. A **957**, 332 (2017).

[21] V. Z. Goldberg and G. V. Rogachev, α-cluster states in N $\neq$ Z nuclei, AIP Conf. Proc. **1491**, 121 (2012).